Fluorescence Studies of the Conformational Dynamics of Parvalbumin in Solution: Lifetime and Rotational Motions of the Single Tryptophan Residue†

Sergio T. Ferreira

Departamento de Bioquimica, Instituto de Ciencias Biomedicas, Universidade Federal do Rio de Janeiro, Rio de Janeiro 21910, Brazil

Received September 21, 1988; Revised Manuscript Received July 21, 1989

ABSTRACT: The fluorescence properties of the single tryptophan residue in whiting parvalbumin were used to probe the dynamics of the protein matrix. Ca^{2+} binding caused a blue-shift in the emission (from λ_{max} = 339 to 315 nm) and a 2.5-fold increase in quantum yield. The fluorescence decay was nonexponential in both Ca^{2+}-free and Ca^{2+}-bound parvalbumin and was best described by Lorentzian lifetime distributions centered around two components: a major long-lived component at 2–5 ns and a small subnanosecond component. Raising the temperature from 8 to 45 °C resulted in a decrease in both the center (average) and width (dispersion) of the major lifetime distribution component, whereas the center, width, and fractional intensity of the fast component increased with temperature. Arrhenius activation energies of 1.3 and 0.3 kcal/mol were obtained in the absence and in the presence of Ca^{2+}, respectively, from the temperature dependence of the center of the major lifetime distribution component. Direct anisotropy decay measurements of local tryptophan rotations yielded an activation energy of 2.3 kcal/mol in Ca^{2+}-depleted parvalbumin and indicated a correlation between rotational rates and lifetime distribution parameters (center and width). Ca^{2+} binding produced a decrease in the width of the major lifetime distribution component and a decrease in tryptophan rotational mobility within the protein. There was a rough correlation between these two parameters with changes in Ca^{2+} and temperature, so that both measurements may be taken to indicate that the structure of Ca^{2+}-bound parvalbumin was more rigid than in Ca^{2+}-depleted parvalbumin.

Parvalbumins are small (M_r ~12 000) water-soluble Ca^{2+}-binding proteins found in significant amounts in fish and amphibian muscle (Hamoir & Konosu, 1965; Pechere et al., 1971, 1973). The crystal structure of carp parvalbumin (Kretsinger et al., 1971; Hendrikson & Karle, 1973; Moews & Kretsinger, 1975) reveals six helical regions which were named A through F. The loop regions between helices C–D and E–F form Ca^{2+}-binding sites (Kretsinger, 1980). Residue 102 in the F helix of whiting parvalbumin is the single tryptophan residue in the protein.

In this report, the effects of temperature and Ca^{2+} binding on the fluorescence lifetimes and on tryptophan anisotropy decay in whiting paravalbumin were investigated, with the goal of trying to correlate the fluorescence decay with the internal dynamics of this protein. For both Ca^{2+}-free and Ca^{2+}-bound parvalbumin, the fluorescence decay was found to be nonexponential. Previous lifetime measurements on parvalbumin have indicated nonexponential decay (Permyakov et al., 1985; Eftink & Wasylewski, 1989), while Castelli and co-workers (Castelli et al., 1988) reported exponential decay for Ca^{2+}–parvalbumin and double-exponential decay for Ca^{2+}-free parvalbumin. Despite some controversy regarding the complexity of the fluorescence decay, the average lifetime of the major decay component reported in these studies increased upon Ca^{2+} binding (Castelli et al, 1988; Eftink & Wasylewski, 1989). In the present work, bimodal Lorentzian lifetime distributions were used to describe the fluorescence decay of parvalbumin, and the behavior of the major lifetime component (which accounted for 83–97% of the fluorescence decay under various experimental conditions) was compared to the rotational mobility of the tryptophan residue. Anisotropy decay measurements showed that Ca^{2+} binding resulted in a significant decrease in the local mobility of the tryptophan residue. Tryptophan rotational rates measured over the temperature range 8–45 °C for both Ca^{2+}-loaded and Ca^{2+}-free parvalbumin indicated a correlation between fluorescence lifetimes and internal mobility in this protein.

Materials and Methods

Emission spectra were obtained on an ISS Inc. (Champaign, IL) GREG 200 spectrofluorometer. Spectral moments (average emission wavelength and standard deviation) were calculated with software provided by ISS Inc. The average emission wavelength was calculated as $\lambda_{av} = \int \lambda I(\lambda)\, d\lambda / \int I(\lambda)\, d\lambda$. The standard deviation was given by st dev = $\int \lambda^2 I(\lambda)\, d\lambda / \int I(\lambda)\, d\lambda$, where λ and $I(\lambda)$ are wavelength (in nanometers) and fluorescence intensity at a given wavelength, respectively.

Lifetimes were measured in a frequency domain fluorometer using the harmonic content of a Coherent Antares Model mode-locked, synchronously pumped, cavity-dumped, and externally frequency doubled dye laser. Excitation was at 295 nm using magic-angle configuration, and the emission was through a WG 320 (Oriel Corp., Stratford, CT) filter. Color errors due to photomultiplier response were minimized by the use of a solution of *p*-terphenyl (Eastman Kodak Co., Rochester, NY) in cyclohexane in the reference cuvette (lifetime of 1.0 ns). Data were acquired at 10 different frequencies from 2 to 200 MHz with uncertainties of ±0.2° and ±0.004 for phase angles and modulation ratios, respectively, and were fitted with a sum of exponential decay components using nonlinear least-squares analysis or as continuous distributions of lifetime values. In both cases, the analysis software provided by ISS Inc. included the above errors in measuring the phase

† Supported by CAPES–Coordenação de Aperfeicoamento de Pessoal de Ensino Superior and FINEP–Financiadora de Estudos e Projetos. The spectrofluorometer in the Departamento de Bioquimica, UFRJ, was purchased with a grant from Conselho Nacional de Desenvolvimento Cientifico e Tecnologico (CNPq/PADCT).

0006-2960/89/0428-10066$01.50/0

Table I: Lifetime Analysis for Ca^{2+}-Free Parvalbumin[a]

	single-exponential fit		double-exponential fit				unimodal Lorentzian fit			bimodal Lorentzian fit					
temp (°C)	τ	χ^2	τ_1	τ_2	f_1	χ^2	c	w	χ^2	c_1	w_1	c_2	w_2	f_1	χ^2
8	3.74	457.90	5.42	1.08	0.83	23.78	4.06	3.43	14.16	4.42	2.35	0.01	0.05	0.97	4.55
14	3.38	441.41	5.02	1.05	0.81	25.08	3.64	3.14	14.15	3.99	2.15	0.01	0.05	0.97	5.04
25	2.85	436.82	4.47	0.99	0.76	19.10	3.01	2.81	12.65	3.38	1.91	0.01	0.05	0.96	3.17
35	2.43	362.63	3.99	0.98	0.71	7.23	2.51	2.25	10.29	2.88	1.48	0.01	0.20	0.95	2.05
45	1.96	328.40	3.36	0.83	0.66	6.25	1.96	1.87	10.51	2.64	0.91	0.52	0.94	0.79	1.41

[a] Fluorescence decay was measured in 50 mM Tris-HCl, pH 7.5, at pCa 9.6. Phase modulation data were fitted with single- or double-exponential models, or with unimodal or bimodal Lorentzian lifetime distributions. The recovered parameters for each analysis are shown. Exponential lifetimes (τ_i), as well as center (c_i) and width (w_i) values in the distribution analysis, are in nanoseconds. Fractional intensities (f_i) were calculated as $f_1 = \alpha_1\tau_1/\sum\alpha_i\tau_i$.

Table II: Lifetime Analysis for Ca^{2+}-Bound Parvalbumin[a]

	single-exponential fit		double-exponential fit				unimodal Lorentzian fit			bimodal Lorentzian fit					
temp (°C)	τ	χ^2	τ_1	τ_2	f_1	χ^2	c	w	χ^2	c_1	w_1	c_2	w_2	f_1	χ^2
8	3.12	346.18	4.07	0.54	0.89	6.47	3.32	2.30	39.54	3.80	0.64	0.01	0.05	0.94	3.88
14	2.98	407.54	3.92	0.39	0.89	6.68	3.15	2.51	42.70	3.71	0.70	0.01	0.05	0.93	1.09
25	2.84	389.01	3.95	0.65	0.85	10.47	3.00	2.44	31.84	3.50	0.97	0.01	0.05	0.94	3.55
35	2.64	336.37	3.51	0.45	0.87	3.48	2.77	2.03	39.77	3.37	0.30	0.01	0.43	0.89	2.17
45	2.41	309.18	3.26	0.49	0.85	1.83	2.50	1.83	35.98	3.23	0.05	0.38	0.64	0.83	1.47

[a] Fluorescence decay was measured in 50 mM Tris-HCl, pH 7.5, at pCa 3. All other conditions as described in the legend to Table I.

delay or modulation for the calculations of χ^2 of the fits. A description of the models and equations used in the analysis of the decay as lifetime distributions and a discussion of the resolvability of the distributions with respect to a sum of exponentials were presented by Alcala et al. (1987a). The ability of the distribution analysis to recover a single-exponential decay (i.e., a distribution with a 0.05-ns width, the low-limit set in our analysis software) was verified by measurements of *N*-acetyl-L-tryptophanamide (NATA)[1] at pH 7. This analysis accurately recovered a lifetime of 3.03 ns with a width of 0.05 ns (not shown), consistent with previous reports (Szabo & Rayner, 1980). Differential phase measurements were done on the same instrument with a polarizer in the emission pathway, and data were fitted with nonlinear least-squares software provided by ISS Inc., as described under Results. Measurements were carried out by using a thermostated sample holder which was flushed with N_2 to avoid condensation.

Whiting parvalbumin was a kind gift of Dr. F. G. Prendergast and was purified by a modification of the method of Closset and Gerday (1971). Samples were >95% pure in isotype IIIb as judged by gel electrophoresis in the presence of SDS or 2 M urea and isoelectric focusing. β-Mercaptoethanol (5 mM) was used throughout the isolation to prevent oxidation of the protein. Castelli et al. (1988) have reported heterogeneous fluorescence of parvalbumin samples that are stored in solution, and that this problem is eliminated by storing lyophilized protein at −20 °C. In the present study, lyophilized samples were stored at −20 °C and were dissolved in 50 mM Tris-HCl, pH 7.5, immediatly before use. $CaCl_2$ or EGTA was added to give the desired free Ca^{2+} concentrations using the Ca^{2+}–EGTA association constants of Schwarzenbach (1957).

Results

Ca^{2+} Effects on the Fluorescence Emission Spectrum. Parvalbumin emission spectrum was recorded at different Ca^{2+} concentrations. At 10^{-7} M Ca^{2+}, the emission spectrum displayed a maximum at 315 nm (Figure 1A, curve a). Addition of increasing concentrations of EGTA to diminish the free Ca^{2+} concentration resulted in a red-shift of the emission spectrum. At 10^{-11} M free Ca^{2+}, the emission displayed a maximum at 339 nm, and a 2.5-fold intensity decrease (Figure 1A, curve c). These results indicate increased tryptophan exposure upon Ca^{2+} removal, and are in line with previous steady-state fluorescence results (Burstein et al., 1975; Permyakov et al., 1980; White, 1988) and with recent reports on the accessibility of the single tryptophan residue to hydrophilic quenchers (Castelli et al., 1988; Eftink & Wasylewski, 1989). Figure 1B shows titration curves of the center of mass (or average emission wavelength) and width (or standard deviation) of the emission spectra obtained as a function of Ca^{2+} concentration. An apparent K_d of 2–6 nM for Ca^{2+} binding to parvalbumin was obtained from the titration of spectral changes shown in Figure 1B, which is in good agreement with previously published values (Pechere et al., 1971; Robertson et al., 1981).

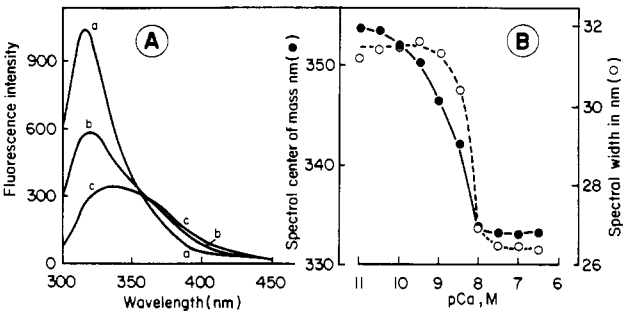

FIGURE 1: (Panel A) Fluorescence emission spectra (excitation at 295 nm) of parvalbumin (3 μM) in 50 mM Tris-HCl, pH 7.5, 25 °C, with the appropriate concentrations of calcium chloride and EGTA to give the indicated free Ca^{2+} concentrations: (a) pCa 7.0, (b) pCa 8.5, (c) pCa 11.0. Excitation and emission slits were 4 nm. Spectra were corrected by subtracting the fluorescence of blanks which did not contain protein. (Panel B) Plot of emission spectral moments [center of mass (●) and width (○)] as a function of free Ca^{2+} concentration.

Ca^{2+} Effects on the Fluorescence Decay. The fluorescence decay of parvalbumin was measured at 25 °C both in the absence and in the presence of Ca^{2+}. In both cases, attempts to fit phase modulation data with a single-exponential did not

[1] Abbreviations: EGTA, [ethylenebis(oxyethylenenitrilo)]tetraacetic acid; NATA, *N*-acetyl-L-tryptophanamide; SDS, sodium dodecyl sulfate; Tris, tris(hydroxymethyl)aminomethane.

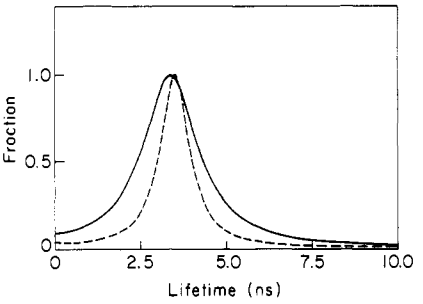

FIGURE 2: Bimodal Lorentzian lifetime distributions for Ca^{2+}-depleted (solid line) or Ca^{2+}-bound (dashed line) parvalbumin at 25 °C.

give satisfactory results, as indicated by the large χ^2 values obtained (Tables I and II). In the absence of Ca^{2+} (Table I), large χ^2 values were also found when data were analyzed with a sum of two exponential components, and a good fit of the data was only obtained with a bimodal Lorentzian distribution of lifetimes. Uniform or Gaussian distribution analysis did not yield good fits of the data (not shown). In the presence of Ca^{2+} (Table II) at 25 °C, it was possible to fit data with a sum of two exponential components (with an χ^2 of 10.47) although a better description of the decay was obtained with bimodal Lorentzian distribution analysis, which yielded an χ^2 of 3.55. The significance of this improvement in fit was evaluated by calculating the *F* statistics of the decrease in χ^2, taking into account the number of degrees of freedom in each fit (Motulsky & Ransnas, 1987). This analysis indicated with a >99% confidence interval that the distribution model was superior to the double exponential in fitting the experimental data. At 25 °C the fluorescence decay of parvalbumin was described by broad distributions of lifetimes, centered at 3.38 and 3.50 ns for Ca^{2+}-free and Ca^{2+}-bound protein, respectively (Tables I and II); in both cases, 96–97% of the fluorescence decay could be described by these major long-lived lifetime distribution components. The remaining 3–4% of the fluorescence intensity appeared to decay as a very fast component centered at 0.01 ns for both Ca^{2+}-loaded and Ca^{2+}-depleted parvalbumin. Since lyophilized samples stored at −20 °C were used throughout this work, it is unlikely that this small fast component was due to partial denaturation of "old" protein in solution which was suggested by Castelli et al. (1988). Furthermore, Castelli et al. (1988) suggested that scattered excitation light could result in the appearance of fast (0.03 ns) decay components. Scattered light does not seem compatible with the fast component observed here, since center, width, and fractional intensities of this component were dependent on the experimental conditions, i.e., temperature and presence or absence of Ca^{2+} (Tables I and II), which suggest that this decay component may originate from different conformational states of the protein. In any case, since the origin of this fast component is not known and it accounts for only 3–17% of the fluorescence decay (Tables I and II), it will not be further pursued here and henceforth we will be mostly concerned with the behavior of the major long-lived distribution component.

Figure 2 shows that the major effect of Ca^{2+} binding to parvalbumin was a decrease in the width of the major lifetime distribution component, with only a small increase in the average lifetime. This is in line with the findings of Eftink and Wasylewski (1989), who reported that Ca^{2+} binding to codfish parvalbumin produced a decrease in the width of the lifetime distribution. No change was detected in the width of the small fast component, which was already at the lower limit set by our analysis software (0.05 ns). In this figure (and also in Figure 3), the peak height of each distribution component is

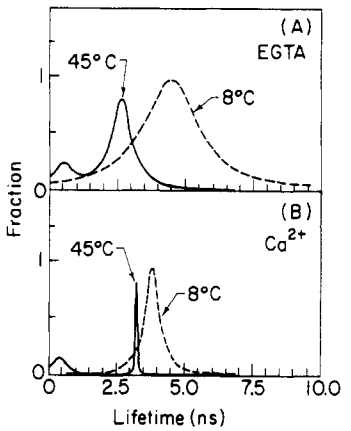

FIGURE 3: Bimodal Lorentzian lifetime distributions for Ca^{2+}-depleted (panel A, pCa 9.6) or Ca^{2+}-bound (panel B, pCa 3) parvalbumin. Dashed lines are at 8 °C and solid lines at 45 °C.

equal to its respective fractional intensity. Thus, the curves are normalized so that the sum of the peak heights of the two components in the bimodal distribution equals 1, as described by Alcala and co-workers (Alcala et al., 1987a–c).

Temperature Dependence of the Fluorescence Decay. Measurements were performed both in the absence and in the presence of Ca^{2+} in the temperature range 8–45 °C to further characterize the fluorescence decay of Ca^{2+}-free and Ca^{2+}-loaded parvalbumin. The results are summarized in Tables I (Ca^{2+}-free parvalbumin) and II (Ca^{2+}-loaded parvalbumin). Single-exponential analysis was unable to fit experimental data over the whole temperature range for both forms of parvalbumin. Analysis of data obtained in the absence of Ca^{2+} with bimodal Lorentzian lifetime distributions yielded better descriptions of the decay than the double-exponential analysis over the temperature range studied (Table I). This was also true for the Ca^{2+}-bound protein in the temperature range 8–25 °C (Table II). For Ca^{2+}-bound parvalbumin above 25 °C, the double exponential and the bimodal distribution analysis gave similar results (Table II).

Figure 3A shows Lorentzian distribution functions obtained in the analysis of Ca^{2+}-free parvalbumin lifetime data at the lowest and highest temperatures tested. At 8 °C, 97% of the fluorescence decay could be described by an extremely broad distribution component centered at 4.42 ns and with a width of 2.35 ns (Figure 3A, dashed line). The remaining 3% of the fluorescence intensity presented a much faster (0.01 ns) decay (Table I). Increasing the temperature to 45 °C resulted in a marked decrease in both center and width of the major lifetime distribution component (Figure 3A). In addition, the width and fractional intensity of the small fast component increased above 25 °C (Table I), and this effect was reversible upon lowering the temperature.

Figure 3B shows Lorentzian distribution functions for Ca^{2+}-bound parvalbumin at the two limits of temperature studied. At 8 °C (Figure 3B, dashed line), 94% of the fluorescence decay could be described by a distribution component centered at 3.80 ns with a width of 0.64 ns (Table II). The remaining 6% of the fluorescence intensity presented a fast (0.01 ns) decay. Increasing the temperature to 45 °C resulted in a decrease in the width of the major distribution component to 0.05 ns (Figure 3B), with a small decrease in its center. Thus, at 45 °C in the presence of Ca^{2+}, the fluorescence decay of parvalbumin was described predominantly by an exponential component of 3.23 ns. Increasing the temperature above 25 °C also caused a reversible increase in width and fractional intensity of the small fast component (Table II).

Table III: Analysis of Parvalbumin Anisotropy Decay Data[a]

	Ca^{2+}-free						Ca^{2+}-bound					
temp (°C)	τ	ϕ_1	r_1	ϕ_2	r_2	χ^2	τ	ϕ_1	r_1	ϕ_2	r_2	χ^2
8	4.06	8.98	0.14	0.53	0.20	2.73	3.31	12.90	0.11	0.64	0.23	5.72
14	3.64	8.60	0.13	0.53	0.21	1.27	3.15	9.61	0.12	0.54	0.21	6.18
25	3.01	5.28	0.12	0.23	0.22	14.78	3.00	7.86	0.16	0.54	0.18	3.16
35	2.51	4.00	0.11	0.24	0.23	4.77	2.77	4.95	0.16	0.51	0.18	2.67
45	1.96	1.82	0.19	0.19	0.14	4.70	2.50	3.05	0.17	0.61	0.14	4.70

[a] Anisotropy decays were measured in 50 mM Tris-HCl, pH 7.5, for either Ca^{2+}-free parvalbumin (pCa 9.6) or Ca^{2+}-bound parvalbumin (pCa 3). Differential phase angles and modulation ratios were fitted with a double-exponential model, with rotational correlation times ϕ_1 and ϕ_2 and preexponential factors r_1 and r_2, respectively. Rotational correlation times are in nanoseconds.

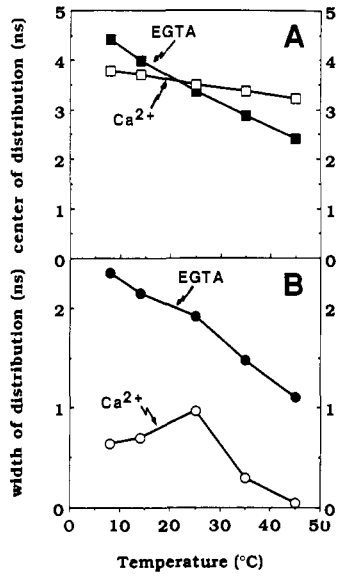

FIGURE 4: Lifetime distribution parameters (center, panel A; width, panel B) for the major component in the bimodal Lorentzian analysis as a function of temperature. Closed symbols, Ca^{2+}-depleted parvalbumin; open symbols, Ca^{2+}-bound parvalbumin. Values from Tables I and II.

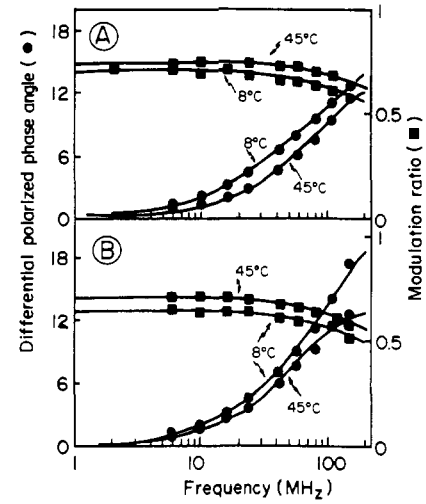

FIGURE 5: Plots of the raw differential polarized phase and modulation data as a function of modulation frequency. (Panel A) Ca^{2+}-depleted parvalbumin, pCa 9.6; (panel B) Ca^{2+}-bound parvalbumin, pCa 3. Solid lines are nonlinear least-squares fits of the data with two rotational correlation times as described under Results.

Figure 4A summarizes the changes in the center of the major distributed lifetime component as a function of temperature both in the absence and in the presence of Ca^{2+}. In the absence of Ca^{2+} (Figure 4A, filled squares), the center of the lifetime distribution decreased continuously as temperature was raised. Binding of Ca^{2+} rendered the distribution center much less sensitive to temperature (open squares).

The temperature dependence of the width of the major lifetime distribution component in both Ca^{2+}-free and Ca^{2+}-bound parvalbumin is shown in Figure 4B. In the absence of Ca^{2+}, the width of the distribution decreased as the temperature was raised from 8 to 45 °C (filled circles). In the presence of Ca^{2+} (open circles), the distribution widths were much narrower than in the absence of Ca^{2+} at all temperatures studied. Furthermore, as the temperature was increased above 25 °C in the presence of Ca^{2+} (open circles), the width decreased down to 0.05 ns, indicating exponential decay.

Temperature Dependence of Tryptophan Rotations in Parvalbumin. The rotational motions of the single tryptophan residue in parvalbumin were investigated by using differential polarized phase fluorometry as described by Weber (1977) in the temperature range 8–45 °C. Data were fitted by assuming that the decay of the anisotropy originated from a single fluorophore with a single lifetime and two discrete rotational correlation times. Attempts to fit data with only one rotational correlation time were not successful (not shown). Since the fluorescence decay of parvalbumin was found to be nonexponential, the center of the Lorentzian lifetime distributions (Tables I and II) was used as an average lifetime value in the rotational analysis. Table III shows the results obtained for the fits of data both in the absence and in the presence of Ca^{2+}. As the χ^2 values in Table III indicate, the decay of the anisotropy could be well described by the model in all experimental conditions.

Figure 5A shows a plot of the raw differential phase angle (closed circles) and modulation (closed squares) data versus frequency for Ca^{2+}-depleted parvalbumin at 8 and 45 °C. Raising the temperature from 8 to 45 °C shifted both curves to higher frequencies. This decrease in frequency–response of both differential phase angles and modulation ratios indicated faster rotational motions of the fluorophore at higher temperature. Solid lines in Figure 5A are fits of the data obtained at 8 and 45 °C. For Ca^{2+}-free parvalbumin at 8 °C, data could be well fitted with two rotational correlation times of 8.98 and 0.53 ns (Table III). It should be noted that a rotational correlation time of 7.4 ns would be expected for the rotation of parvalbumin at 8 °C, assuming a molecular weight of 12000 and a hydration shell of 0.2 g of water/g of protein (Lakowicz, 1983). Therefore, the slow component in the rotational analysis (8.98 ns) probably reflected the overall rotation of the protein in solution, while the fast component (0.53 ns) was most likely associated with local tryptophan motions within the protein matrix. Similar resolution of overall protein rotation and internal tryptophan mobility has been reported for lysozyme (Gratton et al., 1986).

Figure 6A shows the temperature dependence of both slow (open circles) and fast (closed circles) components in the rotation analysis for Ca^{2+}-free parvalbumin. Raising the temperature produced significant decreases in both rotational correlation times, thus indicating increased rates in both overall

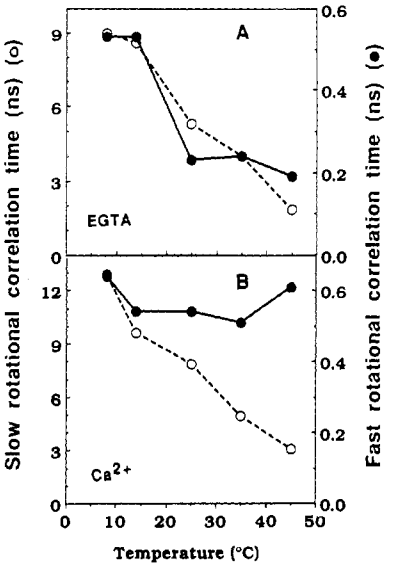

FIGURE 6: Rotational correlation times as a function of temperature (values from Table III). (Panel A) Ca^{2+}-depleted parvalbumin, pCa 9.6; (panel B) Ca^{2+}-bound parvalbumin, pCa 3.

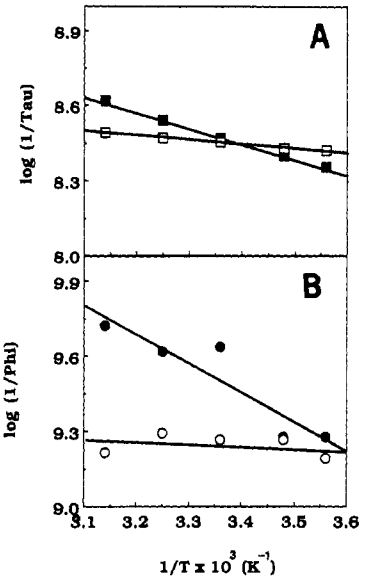

FIGURE 7: Arrhenius plots for the lifetimes (upper panel) and fast rotational correlation times (lower panel). Closed symbols, Ca^{2+}-depleted parvalbumin, pCa 9.6; open symbols, Ca^{2+}-bound parvalbumin, pCa 3.

tumbling of the protein and local tryptophan mobility.

Figure 5B shows multifrequency differential phase (closed circles) and modulation (closed squares) data for Ca^{2+}-bound parvalbumin. At 8 °C, data were fitted (solid lines) with two rotational correlation times of 12.90 and 0.64 ns. Thus, Ca^{2+} binding caused an increase in the overall (slow) rotational correlation time as compared to that obtained in the absence of Ca^{2+} (Table III). Increasing the temperature to 45 °C resulted in decreased overall rotational times (Figure 6B, open circles). However, it should be stressed that the major effect of Ca^{2+} binding on the anisotropy decay was to render the fast rotational time (i.e., local tryptophan mobility) insensitive to temperature (Figure 6B, closed circles).

Activation Energies for Lifetimes and Rotational Mobility. Arrhenius analysis of the temperature dependence of the center of the major lifetime distribution component (Figure 7A) yielded activation energies (E_a) of 1.3 and 0.3 kcal/mol in the absence and in the presence of Ca^{2+}, respectively. The temperature dependence of the fast rotational correlation time (Figure 7B) yielded an E_a of 2.3 kcal/mol in the absence of Ca^{2+} (closed circles), while addition of Ca^{2+} abolished the temperature dependence of the local tryptophan rotational mobility (open circles). Thus, lifetime and anisotropy decay measurements yielded similar activation energies for Ca^{2+}-depleted parvalbumin, while Ca^{2+} binding rendered both parameters little or nondependent on temperature.

Discussion

Analysis of the fluorescence decay of Ca^{2+}-bound or Ca^{2+}-free parvalbumin revealed complex decay kinetics (Tables I and II). The complexity of the decay observed with parvalbumin probably reflected heterogeneity of conformations of the protein matrix, and not an inaccuracy of the measurements since control measurements of the fluorescence decay of NATA accurately yielded a single-exponential lifetime. Recently, a single-exponential lifetime of 4.58 ns was reported for Ca^{2+}-bound parvalbumin at 20 °C (Castelli et al., 1988). In the present work, a major lifetime of 3.95 ns was found in the double-exponential analysis for Ca^{2+}-bound parvalbumin at 25 °C (Table II). Lorentzian distribution analysis showed a major component centered at 3.50 ns (Table II). Thus, there is good agreement between the lifetime values reported here and by Castelli et al. (1988): the double-exponential analysis indicated only 16% difference, and the distribution analysis indicated 30% difference between the present values and those of Castelli et al. (1988). In the absence of Ca^{2+}, Castelli et al. (1988) reported a biexponential decay with a major component of 4.26 ns and a smaller component of 1.28 ns. Here the biexponential analysis at 25 °C yielded lifetimes of 4.47 and 0.99 ns (Table I). Therefore, the major component obtained here in the biexponential analysis differed by only 5% from that reported by Castelli et al. (1988), while the short-lifetime component differed by 30%.

While the average lifetimes reported by Castelli et al. (1988) and here are similar, the complexity of the decay was found to be different in both works. It should be noted that the lifetimes reported by Castelli et al. (1988) were measured at high ionic strength (1 M KCl) whereas in the present report measurements were carried out at low ionic strength (50 mM Tris-HCl). Furthermore, Castelli and co-workers (Castelli et al., 1988) carried out their measurements at pH 9 with 40 μM parvalbumin, whereas pH 7.5 and 3 μM parvalbumin were used throughout the present work. These experimental differences may account for the difference in decay complexity observed by Castelli et al. (1988) and here. In addition, James et al. (1988) pointed out that using the single photon counting technique it is necessary to acquire over 200000 counts in the peak channel to attempt to distinguish between a double-exponential and a distributed model, and that at 20000 counts level in the park channel [the number of counts reported by Castelli et al. (1988)] it is in general impossible to resolve a double-exponential decay from a distribution of lifetimes. In fact, Castelli et al. (1988) pointed out that they could not rule out distributions of lifetime values centered about their average lifetimes. Very recently, Eftink and Wasylewski (1989) reported complex fluorescence decays on the homologous parvalbumin from codfish and described their data with unimodal Lorentzian lifetime distributions. Thus, it could be that although in some conditions the fluorescence decay of parvalbumin can be described by exponentials, the distribution model may provide a better description of the physical system.

Alcala and co-workers (Alcala et al., 1987a–c) used continuous lifetime distributions to describe complex decays in proteins, showing that even single tryptophan proteins presented distributions of lifetimes which could reflect multiple

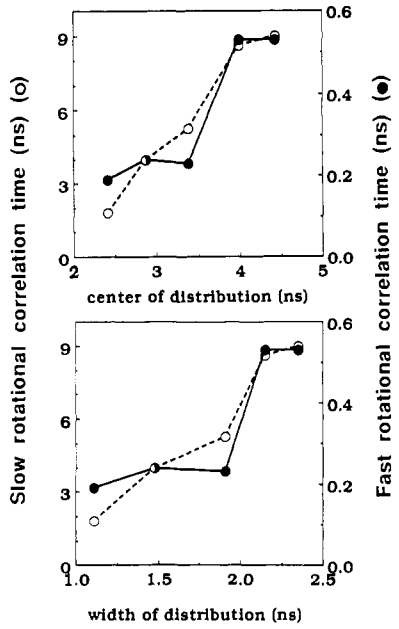

FIGURE 8: Correlation between lifetime distribution parameters (center, upper panel; width, lower panel) and tryptophan rotational correlation times for Ca^{2+}-depleted parvalbumin.

conformational substates of the protein. According to this model, the number of different microenvironments sampled by the tryptophan residue during its excited-state lifetime as well as the rate of interconversion between conformational substates could be expected to affect the fluorescence decay (Gratton et al., 1988). These questions have been addressed in this study by measurements of both lifetimes and fluorescence anisotropy decay of the single tryptophan residue in parvalbumin.

In this work, it is shown that increasing temperature resulted in decreases in the average lifetimes and distribution widths (Figure 4), as well as in the rotational correlation times (Figure 6), suggesting a correlation between these parameters. In Figure 8, the rotational correlation times measured for Ca^{2+}-depleted parvalbumin from 8 to 45 °C (from Table III) were plotted against the distribution parameters (center and width) recovered in the lifetime analysis in the same conditions (from Table I). It is apparent that there is a rough correlation between anisotropy and lifetime parameters, so that increasing lifetimes or distribution widths are associated with an increase in rotational correlation times (i.e., slower rotational motions). Likewise, shorter lifetimes or narrow distribution widths indicate faster rotational motions.

Direct measurements of tryptophan rotations showed that upon Ca^{2+} binding to parvalbumin there was a decrease in rotational mobility (Figure 6B). In fact, the local tryptophan mobility in Ca^{2+}-bound parvalbumin was largely insensitive to temperature (Figure 6B, closed circles), which suggests that the protein matrix surrounding the tryptophan residue was in a much more rigid state in Ca^{2+}-bound parvalbumin than in Ca^{2+}-depleted parvalbumin. Increased tryptophan rigidity should result in a decrease in the number of different microenvironments sampled by the fluorophore, leading to less heterogeneous fluorescence decay. This is entirely in line with the significant decrease in the width of the distributions of lifetimes upon binding of Ca^{2+} (Figures 2 and 3) and gives support to previous correlations between distribution widths and conformational dynamics in proteins (Alcala et al., 1987a–c; Gratton et al., 1988). A similar decrease in the width of the distribution upon Ca^{2+} binding was reported for codfish parvalbumin (Eftink & Wasylewski, 1989), which suggests that in codfish parvalbumin Ca^{2+} binding also results in decreased tryptophan mobility.

In addition to the effects on local tryptophan mobility, Ca^{2+}-induced changes in the shape of parvalbumin were suggested by the increase in the slow rotational correlation times as compared to those obtained in the absence of Ca^{2+} (Table III; Figure 6A,B, open circles). This may indicate that the hydrodynamic radius of Ca^{2+}-bound parvalbumin is larger than that of the Ca^{2+}-free protein or alternatively that the transition moments of tryptophan in Ca^{2+}-bound parvalbumin select a longer rotational time than in the absence of Ca^{2+}.

Arrhenius activation energies of 1.3 and 0.3 kcal/mol were obtained from the temperature dependence of the fluorescence lifetimes in the absence and in the presence of Ca^{2+}, respectively (Figure 7A). Arrhenius analysis of rotational data (Figure 7B) gave an activation energy of 2.3 kcal/mol for Ca^{2+}-depleted parvalbumin, whereas Ca^{2+} binding completely abolished the temperature dependence of the rotational rates. The agreement between the activation energies calculated from lifetime and rotational data further suggests a correlation between parvalbumin lifetimes and internal tryptophan mobility. Recently, Eftink and Wasylewski (1989) reported activation energies of 3 and 2 kcal/mol for the mean lifetime of codfish parvalbumin in the absence and in the presence of Ca^{2+}, respectively. Thus, the decrease in activation energy upon Ca^{2+} binding seems to be a common feature in these two homologous parvalbumins, although this effect was more pronounced in whiting parvalbumin (reported here). This small difference may be due to the difference in position of the tryptophan residue in the two proteins (position 102 in whiting parvalbumin versus position 109 in codfish parvalbumin), which could result in slightly different sensitivity of the tryptophan environment to Ca^{2+} binding.

ACKNOWLEDGMENTS

I thank Drs. Enrico Gratton, Sergio Verjovski-Almeida, and Martha M. Sorenson for many comments and critical reading of the manuscript and Dr. Franklyn G. Prendergast for providing the samples of whiting parvalbumin. All time-resolved fluorescence measurements were performed at the Laboratory for Fluorescence Dynamics (LFD) at the University of Illinois at Urbana—Champaign (UIUC). The LFD is supported jointly by the Division of Research Resources of the National Institutes of Health (RR 03155-01) and UIUC.

Registry No. Ca, 7440-70-2; L-tryptophan, 73-22-3.

REFERENCES

Alcala, J. R., Gratton, E., & Prendergast, F. G. (1987a) *Biophys. J. 51*, 587–596.

Alcala, J. R., Gratton, E., & Prendergast, F. G. (1987b) *Biophys. J. 51*, 597–604.

Alcala, J. R., Gratton, E., & Prendergast, F. G. (1987c) *Biophys. J. 51*, 925–936.

Burstein, E. A., Permyakov, E. A., Emelyanenko, V. I., Bushueva, T. L., & Pechere, J. F. (1975) *Biochim. Biophys. Acta 400*, 1–16.

Castelli, F., White, H. D., & Forster, L. S. (1988) *Biochemistry 27*, 3366–3372.

Closset, J. I., & Gerday, Ch. (1971) *Arch. Int. Physiol. Biochim. 79*, 624–625.

Eftink, M. R., & Wasylewski, Z. (1989) *Biochemistry 28*, 382–391.

Gratton, E., Alcala, J. R., & Marriott, G. (1986) *Biochem. Soc. Trans. 14*, 835–838.

Gratton, E., Silva, N., & Ferreira, S. (1988) in *Biological and Artificial Intelligence Systems* (Clementi, E., & Chin, S.,

Eds.) pp 49-56, ESCOM Science Publishers, Leiden, The Netherlands.
Hamoir, G., & Konosu, S. (1965) *Biochem. J. 96*, 85-97.
Hendrikson, W. A., & Karle, J. (1973) *J. Biol. Chem. 248*, 3327-3334.
James, D. R., Liu, Y.-S., Siemiarczuk, A., Wagner, B. D., & Ware, W. R. (1988) *Proc. SPIE—Int. Soc. Opt. Eng. 909*, 90-96.
Kretsinger, R. H. (1980) *CRC Crit. Rev. Biochem. 12*, 119-174.
Kretsinger, R. H., Dangelat, D., & Bryan, R. F. (1971) *J. Mol. Biol. 59*, 213-214.
Lakowicz, J. R. (1983) *Principles of Fluorescence Spectroscopy*, Pleumn Press, New York.
Moews, P. C., & Kretsinger, R. H. (1975) *J. Mol. Biol. 91*, 201-228.
Motulsky, H. J., & Ransnas, L. A. (1987) *FASEB J. 1*, 365-374.
Pechere, J. F., Demaille, J., & Capony, J. P. (1971) *Biochim. Biophys. Acta 236*, 391-408.
Pechere, J. F., Capony, J. P., & Demaille, J. (1973) *Syst. Zool. 22*, 533-548.
Permyakov, E. A., Yarmolenko, V. V., Emelyanenko, V. I., Burstein, E. A., Closset, J., & Gerday, Ch. (1980) *Eur. J. Biochem. 109*, 307-315.
Permyakov, E. A., Ostrovsky, A. V., Burstein, E. A., Pleshnov, P. G., & Gerday, Ch. (1985) *Arch. Biochem. Biophys. 240*, 781-792.
Robertson, S. P., Johnson, J. D., & Potter, J. D. (1981) *Biophys. J. 34*, 559-569.
Schwarzenbach, G. (1957) *Complexometric Titrations*, Interscience, New York.
Szabo, A. G., & Rayner, D. M. (1980) *J. Am. Chem. Soc. 102*, 554-563.
Weber, G. (1977) *J. Chem. Phys. 66*, 4081-4091.
White, H. D. (1988) *Biochemistry 27*, 3357-3365.

The Nature of Protein Dipole Moments: Experimental and Calculated Permanent Dipole of α-Chymotrypsin

Jan Antosiewicz[‡] and Dietmar Porschke*
Max-Planck-Institut für biophysikalische Chemie, D-3400 Göttingen, FRG
Received January 25, 1989; Revised Manuscript Received July 28, 1989

ABSTRACT: The electric dichroism of α-chymotrypsin has been measured in buffers of various pH values and ion compositions. The stationary dichroism obtained as a function of the electric field strength is not compatible with an induced dipole mechanism and clearly shows that α-chymotrypsin is associated with a substantial permanent dipole moment. After correction for the internal directing electric field according to a sphere model, the dipole moment is 1.6×10^{-27} C m at pH 8.3 (corresponding to 480 D). This value decreases with decreasing pH (to 1.2×10^{-27} C m at pH 4.2), but is almost independent of the monovalent salt concentration in the range from 2 to 12 mM and of Mg^{2+} addition up to 1 mM. The assignment of the permanent dipole moment is confirmed by analysis of the dichroism rise curves. The dichroism decay time constants of (31 ± 1) ns at 2 °C can be represented by a spherical model with a radius of 25-26 Å, which is consistent with the known X-ray structure. The limiting linear dichroism is slightly dependent on the buffer composition and demonstrates subtle variations of the protein structure. As a complement to the experimental results, electric and hydrodynamic parameters of α-chymotrypsin have been calculated according to the known X-ray structure. Bead model simulations provide the center of diffusion, which is used to calculate dipole moments according to the equilibrium charge distribution evaluated from standard p*K* values. In addition, dipole moments are also calculated according to the Tanford-Kirkwood model, which is modified by a more detailed consideration of solvation energies and evaluated from an equilibrium distribution of protein states generated by Monte Carlo techniques. The static dipole moment obtained by the first procedure is consistent with the experimental results over the whole pH range investigated, whereas the Monte Carlo results agree with the experimental data from pH 8.3 to 5.7. The fluctuating dipole moment evaluated by the second procedure gives rise to a minor contribution only, which is usually less than 20% of the static dipole moment. In summary, experimental and theoretical results are in satisfactory agreement and demonstrate the existence of a substantial "true" permanent dipole moment associated with α-chymotrypsin.

The assessment of electric properties for biological macromolecules proved to be particularly difficult—mainly due to the fact that these molecules usually bear a large number of charged residues. In most cases these residues attract counterions, which form a counterion atmosphere with a particularly high polarizability and thus cause large contributions to the measured electric properties. Although the polarization of counterions should be reflected by an induced dipole moment, the case of DNA double helices (Diekmann et al., 1982; Porschke, 1985) demonstrates that special mechanisms may simulate the existence of a permanent dipole moment. Another problem results from site binding of ligands, which compensate the charges attached to the polymer. Usually the extent of site binding is not exactly known. Because of the large dimensions of macromolecules, the contribution of single charged residues may be important for the overall dipole moment. Furthermore, ligand binding at individual sites may fluctuate,

[‡]Present address: Institute of Experimental Physics, Department of Biophysics, University of Warsaw, 02-089 Warsaw, Poland.

0006-2960/89/0428-10072$01.50/0